Proceedings of the International Symposium on Physics of Materials (ISPMA 14), September 10–15, 2017, Prague

Discontinuous Flow of Fine Grained AZ31 at Extremely Low Temperature

N.V. Isaev[a], S.E. Shumilin[a], P.A. Zabrodin[a], M. Janeček[b,*] and J. Stráská[b]

[a]Verkin Institute for Low Temperature Physics and Engineering of the National Academy of Sciences of Ukraine, 47 Nauky Ave., Kharkiv, 61103, Ukraine

[b]Department of Physics of Materials, Faculty of Mathematics and Physics, Charles University, Prague, Czech Republic

The plastic deformation of polycrystals of magnesium alloy AZ31 with microstructures after severe plastic deformation and annealing deformed in tension at a temperature of 0.52 K was studied. It is established that, regardless of the microstructure, the plastic flow is discontinuously exhibiting stress jumps, whose amplitude increases with increase of strain. With increase of grain size due to annealing, the strength of a polycrystalline material decreases, its plasticity increases, and the discontinuous plastic flow is partially suppressed (the jump amplitude is reduced or even disappears). An analysis of the discontinuous flow statistics showed that in ultrafine grained polycrystals the frequency distribution of the stress jump amplitudes is sharper than that of their coarse-grained counterparts. The results of experiments are discussed employing the concept of the avalanche-like dynamics of dislocations being the cause of discontinuous plastic deformation under conditions of low temperatures and high stresses.

DOI: 10.12693/APhysPolA.134.662

PACS/topics: strain hardening, discontinuous flow, low temperatures, magnesium alloy

1. Introduction

The instability of plastic deformation of metals and alloys at cryogenic temperatures is one of the examples of discrete thermally activated stress relaxation in solids. In polycrystalline materials, local stress relaxation is considered to be the result of the avalanche motion of dislocations and a local lattice shear, and is accompanied by jumps (bursts) of the deformation stress, by the release of AE signal, electric potential [1] and subsequent local (adiabatic) heating [2, 3]. With increase of strain, the stress increases until the next jump occurs. As a result, the stress–strain curve exhibits a serrated form, the phenomenon being known as the low-temperature jump-like deformation (LTJD). According to the review [4], where the results of macroscopic experiments with single- and polycrystals of various metals and alloys are discussed, this phenomenon was usually observed in a limited range of temperatures and deformation rates, indicating its thermally activated nature. Moreover, it was found that the scale and the statistics of stress jumps depend on the type of the crystal lattice, the shape, the defect structure and the electronic state of the specimen, as well as on other factors that affect the evolution of the dislocation system and determine the strain hardening rate of the material. Recently the study of the nature of LTJD has been closely associated with the development of methods of severe plastic deformation, which makes it possible to investigate the discontinuous flow of polycrystals with a substantially altered microstructure [5].

*corresponding author; e-mail: janecek@met.mff.cuni.cz

The aim of this study is to investigate the influence of microstructure on the scale and statistics of the discontinuous flow of magnesium alloy AZ31. Polycrystals with a different microstructure: (i) after equal-channel angular pressing and (ii) after subsequent annealing were deformed in tension at a constant strain rate at extremely low temperature.

2. Material and the experimental procedure

Commercial Mg alloy AZ31 polycrystals having the nominal composition (in wt%) Mg-3% Al-1% Zn (Mg-2.7 at.% Al-0.4 at.% Zn) were used in this study. The as cast material was first extruded (EX) at the temperature of 623 K employing the extrusion ratio of 22. The rectangular billets of the cross-section of 10×10 mm^2 and the length of 120 mm were processed by equal-channel angular pressing (ECAP) by 8 passes via route B_C at 453 K; for details of this two-step procedure consisting of hot extrusion followed by ECAP (EX-ECAP), see [6]. Flat specimens for tensile tests having the cross-section of 0.5×3 mm^2 and the gauge length of 15 mm were machined by electrical spark cutting from ECAP billets parallel to the direction of extrusion. Before deformation and structural investigation, the surface of the samples was mechanically polished with emery papers and etched in the solution of 1% (HNO_3)+ 99% (C_2H_6O). The coarse grained (CG) material was prepared by annealing of ECAPed specimens at the temperature of 573 K for 4 h in protective argon atmosphere.

The microstructure of polycrystals after EX-ECAP and annealing was characterized in detail by electron backscatter diffraction (EBSD), transmission electron microscopy (TEM), positron annihilation spectroscopy

(PAS), X-ray diffraction (XRD), and optical microscopy in our previous study [6]. It was shown that the material after 8 ECAP passes (hereinafter referred to as A) consisted of equiaxed grains of the average size of $d_A \approx 0.8$ μm (Fig. 1a).

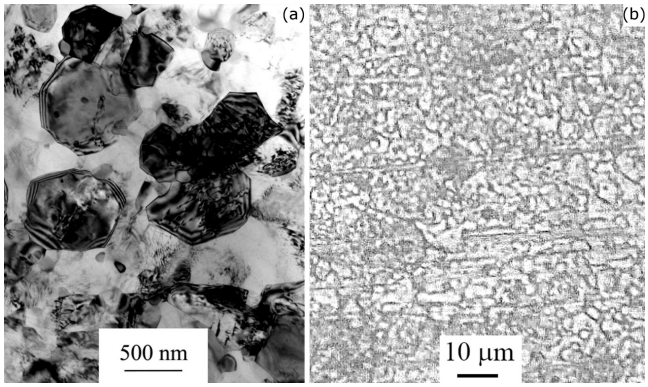

Fig. 1. Microstructure of samples of AZ31: (a) after EX-ECAP [6] (TEM) and (b) after annealing at 573 K (optical microscopy).

According to the PAS and XRD data the average dislocation density ρ_A inside the grains is of the order of $\approx 10^{14}$ m^{-2}.

According to [7], the ultra fine grained (UFG) structure of AZ31 after EX-ECAP, is stable up to the temperature of approximately 523 K. In order to achieve a significant change in the microstructure, the UFG specimen was annealed at the temperature of 573 K for 4 h. As a result, the average grain size in the annealed polycrystalline sample (hereinafter referred to as B) increased to $d_B \approx 2$–3 μm (Fig. 1b), and the average dislocation density decreased to $\rho_B \approx 10^{12}$ m^{-2} (more than ten times compared to ρ_A).

Both UFG (specimen A) and CG (specimen B) specimens were deformed in tension in a specially designed ^{3}He cryostat, using the initial strain rate of $\dot{\varepsilon} = 10^{-4}$ s^{-1}. The constant sample temperature of 0.52 ± 0.02 K in liquid ^{3}He was maintained by adjusting the evacuation of ^{3}He vapors by means of an absorption pump cooled with liquid ^{4}He. Details of the experiment and the characteristics of the apparatus for deformation at extremely low temperatures are described elsewhere [8]. The registered "load–time" signal was subsequently converted into the coordinates "true stress σ–true strain ε". The sensitivity of the apparatus allows to recognize stress jumps with an amplitude of $\Delta\sigma \geq 0.2$ MPa.

3. Results and discussion

The typical serrated tensile curves of A and B specimens of AZ31 polycrystals at the temperature of 0.52 K are shown in Fig. 2. One can see that the specimen B exhibits significantly lower yield stress than the specimen A (110 MPa and ≈ 230 MPa, respectively) and higher ductility. Similarly to room temperature, these differences may be ascribed to the reduced grain size and enhanced density of defects (mainly dislocations) in UFG materials as compared to its CG (annealed) counterpart. In contrast to curve A, the curve B is not parabolic, and the work hardening coefficient $\theta \equiv \partial\sigma \,/\, \partial\varepsilon$ is changing with strain nonmonotonously (see also the inset in Fig. 2).

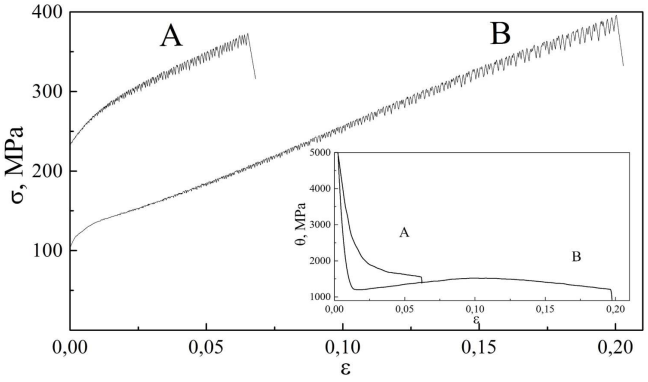

Fig. 2. True stress σ–true strain ε curves of polycrystalline of AZ31: A (EX-ECAP) and B (EX-ECAP + annealed at 573 K). In the inset: the dependence θ–ε, where θ — the work hardening coefficient – is displayed.

Near the yield stress the plastic deformation of samples A and B ceases to be macroscopically stable (smooth), both curves exhibit stress jumps with amplitudes $\Delta\sigma$ in the range of 0.2–20 MPa.

The stress jumps evolution with strain of specimens A and B is illustrated in Fig. 3. It can be seen that for both specimens the average value of the amplitude $\Delta\bar{\sigma}$ monotonously increases with increase of strain. The specimen A exhibits the linear dependence of $\Delta\bar{\sigma}(\varepsilon)$ (dotted line), whereas for specimen B two lines of different slopes seem to be better approximation regardless of a large scatter of data. The slope of the linear approximation $\Delta\bar{\sigma}(\varepsilon)$ for the specimen B changes at the strain of approximately $\varepsilon \approx 0.12$ (Fig. 3), which roughly corresponds to the maximum of the $\theta(\varepsilon)$ dependence (cf. Fig. 2).

In the discussion of the discontinuous flow we will take into account that the plastic deformation of crystals is intrinsically discrete due to its dislocation nature and heterogeneous internal stress. Therefore, an individual avalanche from several dozens of dislocations can originate in the region of stress concentrations, for example, in the head of the dislocation pile-up near a sessile (Frank) dislocation [1, 3–5]. In the case of collapse of this sessile configuration a local excess of mobile dislocations generates a local strain event usually accompanied by the acoustic emission events [4, 9, 10]. However, an individual dislocation avalanche is not powerful enough to provide a visible jump of the flow stress. The macroscopic plastic instability in the form of stress jump $\Delta\sigma$ requires that an individual avalanche triggers other surrounding avalanche events, providing so-called clustering or synchronization of dislocation avalanches and the collective displacement of a significant number

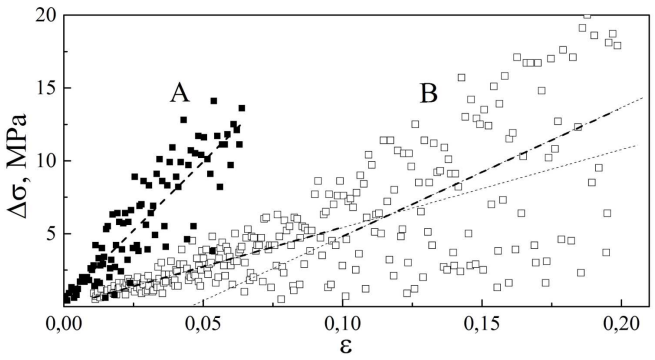

Fig. 3. The dependence of the stress jump amplitude $\Delta\sigma$ on the deformation for A and B AZ31 polycrystals. Dotted lines — the average amplitude $\Delta\bar{\sigma}$.

of dislocations [9–11]. At sufficiently low temperatures, the avalanche-like stress relaxation caused by the displacement of ($\approx 10^3$–10^5) dislocations is considered to be the main mechanism, since other thermally-activated mechanisms (e.g. cross slip) become unlikely [12, 13].

The amplitude $\Delta\sigma$ reflects, in the first approximation, the scale of the catastrophic local shear (the instability scale), which at constant strain rate depends on the dislocation density and the grain size. According to [10], at the early stage of deformation the probability, that the dislocation avalanches generated in the regions of local stress concentrations trigger other surrounding avalanche events (so-called synchronization) giving rise to stress serrations of amplitude $\Delta\sigma$, is determined by the dislocation density. An increase of the total dislocation density (including sessile dislocations) during plastic deformation leads to an increase of the scale of avalanche events and the jumps amplitude $\Delta\sigma$. This explains the higher values of $\Delta\sigma$ observed in UFG sample A processed by EX-ECAP, as compared to the annealed one B, cf. Fig. 3. Due to the same reason the stress–strain curve of sample B is "smooth" at small ε (see Fig. 2), and stress jumps $\Delta\sigma \geq 0.2$ MPa (test sensitivity) are observed only after some critical plastic deformation at work hardening rate reflecting the storage rate of dislocations.

Two effects of the work hardening on the development of plastic instabilities have been recently discussed in [11]. Firstly, the increase of number of obstacles (e.g. sessile configurations) to dislocation motion prevents the mobilization of dislocations and thus inhibits the process of synchronization. This change leads to the diminishing of the frequency of large stress jumps $\Delta\sigma$. Secondly, due to the same reason both an increase and homogenization of internal stresses occurs. Additionally, the density of the mobile dislocations increases with strain. Both these factors can finally create conditions for strong synchronization of dislocation avalanches and result in the occurrence of larger stress jumps.

It should be noted that this assumption does not include the role of grain size in the accumulation and distribution of dislocations at plastic deformation and the scale of plastic instabilities. As a rule, after severe plastic deformation the strength of polycrystals at room temperature increases but the ductility decreases due to decrease of work hardening rate and early necking at tension of the fine grained samples. The lower is the test temperature, the smaller is the critical grain size when a significant loss of ductility is observed. An increase of dislocation density and the fraction of grain boundaries due to EX-ECAP processing at elevated temperatures do not suppress the low temperature work hardening capacity of the fine grained sample A as compared to the coarse grained one B; only the ductility of specimen A is reduced, as seen in Figs. 2 and 3. At the same time, the majority of $\Delta\sigma$ jumps and the slope of the average value $\Delta\bar{\sigma}$ vs. ε are higher in specimen A than in B. In terms of the model [11] large values of $\Delta\sigma$ and fast increase of $\Delta\bar{\sigma}$ with deformation may be explained by the increase of internal stresses and mobile dislocation density as a prevalent effects of low temperature work hardening of the fine grained sample A. The scale of plastic deformation instabilities is limited by low ductility and relatively high work hardening rate of sample A. The grain refinement up to ≈ 0.8 μm does not influence significantly the work hardening mechanism of specimen A as compared to B. The low ductility of UFG specimen A processed by EX-ECAP may be attributed to microstructure properties which do not affect directly the capacity to dislocation storage at low temperatures, e.g. enhanced porosity, small grain size or phase distribution, etc.

The microstructure of the annealed specimen B is characterized by lower dislocation density and bigger average grain size as compared to the initial microstructure of the specimen A. As a result, the flow stress decreases and the ductility increases due to the work hardening coefficient which remains positive up to large deformations. This indicates a change in the dislocation storage mechanism, usually related to more intensive accumulation of dislocations in coarse grains. According to [14], the multiplication of deformation induced obstacles leads to the reduction of the dislocation free path resulting in the suppression of the process of avalanche synchronization. The week dependence of work hardening coefficient θ on ε at large deformations correlates well with the lower slope of $\Delta\bar{\sigma}$ vs. ε and lower frequency of large jumps $\Delta\sigma$ in specimen B as compared to A. The non-monotonous dependence of $\theta(\varepsilon)$ and the variation of the slope $\Delta\bar{\sigma}(\varepsilon)$ near $\varepsilon \approx 0.12$ observed in Fig. 2 and Fig. 3, respectively for the specimen B, indicate the more complex correlation nature of work hardening and discontinuous plastic deformation at low temperatures in the CG specimen B as compared to its UFG counterpart A. One may assume that the observed complex correlation in CG specimen involves the distribution of large grains in the bulk of the specimen B as a factor of inhomogeneous dislocation storage affecting the development of avalanche-like dislocation movement.

The enhanced ductility at extremely low temperatures allows to register sufficiently high number of stress jumps

(of the order of hundreds) on stress–strain curves of both specimens (Fig. 3), providing the opportunity to examine the influence of the microstructure on the statistics of discontinuous flow of the alloy. In order to analyze different strain dependences of average events for samples A and B in a more detail, the corresponding frequency distributions of normalized stress jumps, $\Delta\sigma/\Delta\bar{\sigma}(\varepsilon)$, are shown in Fig. 4.

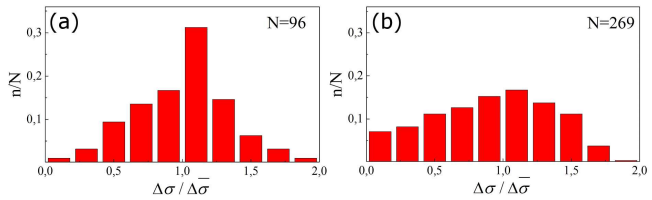

Fig. 4. Frequency distributions of normalized stress jumps $\Delta\sigma/\Delta\bar{\sigma}$ for AZ31 samples of type A (a) and B (b) deformed in tension at the temperature of 0.52 K; N being the total number of jumps.

The statistical data reflect a different dispersion of jumps amplitude in fine grained specimen A and a coarse grained specimen B. Assuming the Gaussian approximation, the half-width of the distribution in A and B specimens being 0.44 and 1.13, respectively. A similar effect of the grain size on the statistics of discontinuous flow at low temperatures was previously observed in aluminum [15] and copper polycrystals [14] subjected to severe plastic deformation and subsequent annealing.

Our experimental data for AZ31 alloy are consistent with the assumptions in [11] about the influence of the deformation stress, determined by the grain size and the dislocations density on the discontinuous plastic deformation. Indeed, the normalized distribution in specimen A illustrates the lower frequency of small and large jumps relative to peak frequency amplitude. The higher internal stress due to grain refinement, the elevated initial dislocation density and fast dislocation storage (large θ) lead to the strong synchronization of individual dislocation events, i.e. to relatively low frequency of small jumps in specimen A. Moreover, the loss of the large jumps may be explained by limited ductility of sample A. On the other hand, according to [1] and reviews [4, 11], the grain boundaries as strong obstacles for dislocations suppress catastrophic dislocation events of scale larger than the average boundary separation.

Another aspect which should be taken into account are the inertial properties of dislocations [16]. It is well known that inertial effects are amplified at low temperatures (due to reduced phonon friction) and high flow stresses (due to grain sizes refinement) [17, 18]. Both effects lead to an increase of the mean free path of dislocations. The enhanced dislocation mobility at low temperatures facilitates the development of dislocation avalanches and affect the statistics of discontinuous plastic deformation particularly in UFG materials.

4. Conclusions

The influence of microstructure (UFG vs. CG state) on the plastic deformation of Mg alloy AZ31 at extremely low temperatures of 0.52 K was investigated. The following conclusions may be drawn from this study:

- the plastic flow was found to be discontinuous in both microstructure conditions,
- the amplitude of stress jumps increases with increase of strain,
- the strength of the UFG specimen was superior and the ductility inferior to that of its CG counterpart,
- the average scale of discontinuous plastic flow in UFG material is larger than in the CG material,
- the dispersion of stress jump amplitudes was higher in the UFG as compared to CG material,
- avalanche-like dislocation dynamics was assumed to be the cause of discontinuous plastic flow in AZ31 alloy at extremely low temperatures.

Acknowledgments

This work was financially support by ERDF under the project CZ.02.1.01/0.0/0.0/15_003/0000485.

Partial financial support by Czech Science Foundation under the project GB 14-36566G is also gratefully acknowledged.

References

[1] V.S. Bobrov, M.A. Lebedkin, *Fiz. Tverd. Tela* **31**, 120 (1989) [*Sov. Phys. Solid State* **31**, 982 (1989)].

[2] A.M. Dolgin, V.Z. Bengus, *Fiz. Nizk. Temp.* **16**, 254 (1990) [*Sov. J. Low Temp. Phys.* **16**, 141 (1990)].

[3] B. Skoczen, J. Bielski, S. Sgobba, D. Marcinek, *Int. J. Plasticity* **26**, 1659 (2010).

[4] V.V. Pustovalov, *Fiz. Nizk. Temp.* **34**, 871 (2008) [*Low Temp. Phys.* **34**, 683 (2008)].

[5] N.V. Isaev, S.E. Shumilin, P.A. Zabrodin, V.G. Geidarov, T.V. Grigorova, V.S. Fomenko, I.S. Braude, V.V. Pustovalov, *Fiz. Nizk. Temp.* **39**, 818 (2013) [*Low Temp. Phys.* **39**, 633 (2013)].

[6] M. Janecek, S. Yi, R. Kral, J. Vratna, K.U. Kainer, *J. Mater. Sci.* **45**, 4665 (2010).

[7] J. Stráská, M. Janeček, J. Čížek, J. Stráský, B. Hadzima, *Mater. Character.* **90**, 69 (2014).

[8] I.N. Kuzmenko, V.V. Pustovalov, *Cryogenics* **25**, 346 (1985).

[9] A.S. Argon, *Philos. Mag.* **93**, 3795 (2013).

[10] B. Obst, A. Nyilas, *Mater. Sci. Eng.* **137**, 141 (1991).

[11] N.P. Kobelev, M.A. Lebyodkin, T.A. Lebedkina, *Met. Mater. Trans. A* **48A**, 965 (2017).

[12] V.P. Lebedev, V.S. Krylovskiĭ, S.V. Lebedev, S.V. Savich, *Phys. Solid State* 49, 2091 (2007).

[13] V.V. Demirski, S.N. Komnik, *Acta Metal.* **30**, 2227 (1982).

[14] N.V. Isaev, T.V. Grigorova, S.E. Shumilin, S.S. Polishchuk, O.A. Davydenko, *Low Temp. Phys.* **43**, 1420 (2017).

[15] S.E. Shumilin, N.V. Isaev, P.A. Zabrodin, V.S. Fomenko, T.V. Grigorova, V.G. Geidarov, *Acta Phys. Pol. A* **128**, 536 (2015).

[16] C.J. Pérez, A. Corral, A. Díaz-Guilera, K. Christensen, A. Arenas, *Int. J. Mod. Phys. B* **10**, 1111 (1996).

[17] A.V. Granato, *Phys. Rev.* **B4**, 2196 (1971).

[18] M.I. Kaganov, V.Ya. Kravchenko, V.D. Natsik, *Usp. Fiz. Nauk* **111**, 655 (1973).